Magnetic field dependence of Pauli spin blockade: A window into the sources of spin relaxation in silicon quantum dots

G. Yamahata,[1,2] T. Kodera,[1,3,4] H. O. H. Churchill,[2] K. Uchida,[5] C. M. Marcus,[2,*] and S. Oda[1]

[1]*Quantum Nanoelectronics Research Center, Tokyo Institute of Technology, 2-12-1 O-okayama, Meguro-ku, Tokyo 152-8552, Japan*

[2]*Department of Physics, Harvard University, Cambridge, Massachusetts 02138, USA*

[3]*Institute for Nano Quantum Information Electronics, The University of Tokyo, Tokyo 153-8505, Japan*

[4]*PRESTO, Japan Science and Technology Agency (JST), 4-1-8 Honcho Kawaguchi, Saitama, Japan*

[5]*Department of Physical Electronics, Tokyo Institute of Technology, 2-12-1 O-okayama, Meguro-ku, Tokyo 152-8552, Japan*

(Received 29 November 2011; revised manuscript received 18 July 2012; published 13 September 2012)

We investigate spin relaxation in a silicon double quantum dot via leakage current through Pauli blockade as a function of interdot detuning and magnetic field. A dip in leakage current as a function of magnetic field on an ∼40 mT field scale is attributed to spin-orbit mediated spin relaxation. On a larger (∼400 mT) field scale, a peak in leakage current is seen in some, but not all, Pauli-blocked transitions, and is attributed to spin-flip cotunneling. Both dip and peak structure show good agreement between theory and experiment.

DOI: 10.1103/PhysRevB.86.115322 PACS number(s): 72.25.Dc, 72.80.Cw, 73.63.Kv

I. INTRODUCTION

Electron spins confined in semiconductor quantum dots (QDs) are attractive candidates for quantum information processing.[1] Coherent manipulation of individual and coupled electron spin states has been mainly investigated in GaAs-based double QD (DQD) devices.[2–4] However, nuclear spins of the host material cause decoherence of the electron spin via strong hyperfine coupling.[5] To reduce this effect, group IV materials, such as carbon, silicon (Si), and silicon-germanium (SiGe), have been investigated[6–10] because their most abundant isotopes have zero nuclear spin. Silicon systems, in particular, have an advantage for future integration because of their compatibility with conventional Si metal-oxide-semiconductor devices.

Toward spin qubits in Si systems, it is necessary to understand the spin relaxation mechanism. Pauli spin blockade (PSB)[11,12] is a valuable tool for investigating spin relaxation in confined systems. In DQDs of several materials, the spin relaxation mechanism has been characterized by analyzing the leakage current in the PSB regime,[13–16] where hyperfine interaction and/or spin-orbit interaction dominate the spin relaxation. For Si systems, a PSB has been reported for a DQD in metal-semiconductor-oxide structures and an electrostatically formed DQD in Si/SiGe heterostructures.[17,18] However, the relaxation mechanism in Si DQDs has not yet been experimentally clarified. More recently, magnetic field dependences of the leakage current in a PSB regime have been demonstrated in a pure Si DQD,[19] where a current peak was explained by field-dependent cotunneling.

In this work, we investigate leakage current in a PSB regime using a lithographically defined Si DQD. By changing magnetic field, we observed a dip of the leakage current at zero magnetic field, presumably the result of spin-orbit-mediated spin relaxation. In addition, magnetic field dependences at a different charge triple point exhibit a leakage current peak at zero magnetic field. This peak can be understood as a signature of spin-flip cotunneling processes.

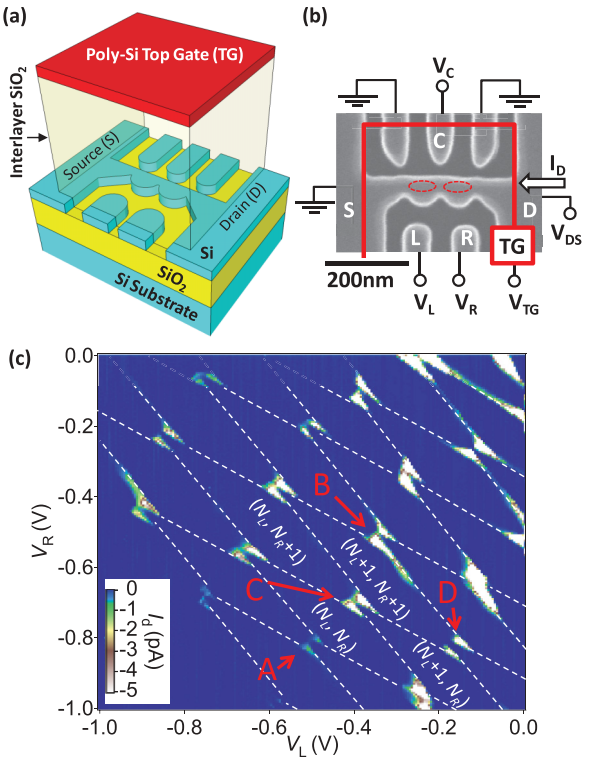

FIG. 1. (Color online) (a) Schematic of the silicon double quantum dot (Si DQD). (b) Scanning electron microscope image of the Si DQD before the top gate formation. The two side gates located next to side gate C are grounded. (c) Charge stability diagram of the Si DQD as a function of V_L and V_R at zero magnetic field, where $V_{ds} = -2$ mV, $V_{TG} = 0.90$ V, and $V_C = -1.72$ V. The white dotted lines are boundaries of the stable charge states. The charge numbers in the left and right QDs are N_L and N_R, respectively.

II. DEVICE AND MEASUREMENT SCHEME

Figure 1(a) shows a schematic of a Si DQD. Three constrictions between the source (S) and drain (D), and five side gates

were patterned by electron beam lithography on a 60-nm-thick (100) Si-on-insulator (SOI) layer, where the thickness of the buried oxide was 400 nm. Reactive ion etching was used to transfer the resist pattern onto the SOI, followed by formation of the gate oxide via thermal oxidation for 30 min at 1000 °C and low-pressure chemical vapor deposition (LPCVD). Then, a wide poly-Si top gate (TG) formed by LPCVD was used as an ion implantation mask for the formation of the n-type S and D regions. Finally, 300-nm-thick aluminum contact pads were formed by electron beam evaporation. Figure 1(b) shows a scanning electron microscope image of the device, where the DQD is defined by tunnel barriers at the three constricted regions.[20]

Electrons were attracted to the Si (100) surface by applying a positive TG voltage, V_{TG}. Electrochemical potentials of the left and right QDs were modulated by applying voltages V_{L} and V_{R} to side gates L and R. The tunnel coupling between the two QDs was controlled by voltage V_{C} applied to side gate C. All measurements were carried out in a ^{3}He refrigerator with a base temperature of 250 mK.

III. RESULTS AND DISCUSSION

A. Transport measurements

The honeycomb charge stability [Fig. 1(c)] reflects the formation of a DQD.[21] Charging energies of the left and right QDs were estimated to be 10.7 and 11.0 meV, respectively, from the spacings of the Coulomb peaks, implying that the QDs have almost the same size. In addition, from the distribution of the current peaks due to resonant tunneling at triple point A in Fig. 1(c), the quantum level spacing, ΔE, of the left and right QD was estimated to be 310 and 260 μeV, respectively [for example, see Fig. 4(b) for the right QD]. In confirmation, ΔE can be approximated as $\Delta E = h^2/8\pi m^* A$, where m^* gives effective mass here, h is Planck's constant, and A is the area of the QD,[22] with spin and valley degeneracies included. This equation determines ΔE to be between 260 and 380 μeV for our device geometry, in good agreement with the experimental estimation. We conclude that the QD is formed between the two constricted regions indicated by the ovals in Fig. 1(b).

Current rectification in DQDs due to a PSB appears at a triple point with only one bias polarity.[12] We observed such current rectification with a negative bias voltage at triple point B in Fig. 1(c), as indicated by the trapezoid in Fig. 2(a), whereas no current rectification appeared with positive bias as shown in Fig. 2(b). In addition, the current rectification is lifted along the outer edge of the PSB regime indicated by the circle in Fig. 2(a) because of electron exchanges between the DQD and the right lead, comparable to PSB seen in GaAs DQDs.[12]

Since Si DQDs normally have doubly degenerate valleys due to confinement in the direction perpendicular to the Si surface, the valley degeneracy could lift a PSB. However, the fact that a PSB is observed indicates either a lifting of valley degeneracy or weak tunneling between valleys.[23] In the former case, once two spins occupy the (1, 1) triplet state as shown in Fig. 2(c), the current flow is suppressed due to the PSB until relaxation from (1, 1) triplet to (1, 1) singlet occurs. In the latter case, even if degenerate valleys exist as shown in Fig. 2(d), the PSB is not lifted because intradot and interdot tunnelings between valleys are weak.

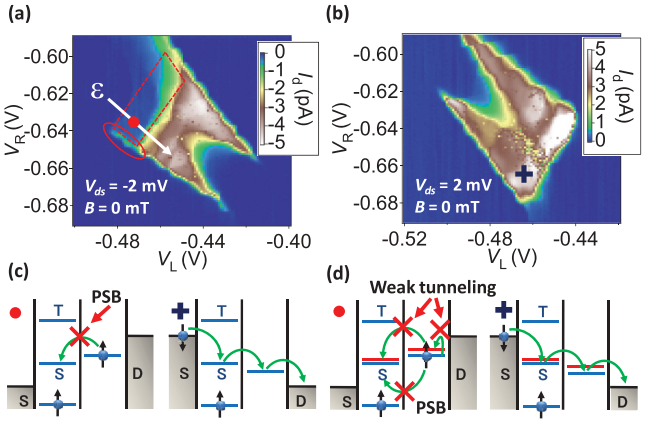

FIG. 2. (Color online) (a) Triple point B shown in Fig. 1(c) with negative bias, where $V_{\mathrm{ds}} = -2$ mV, $V_{\mathrm{TG}} = 0.97$ V, and $V_{\mathrm{C}} = -1.76$ V. The PSB appears only for this polarity. Here ϵ is the detuning axis. (b) The same triple point as in (a) under a positive bias ($V_{\mathrm{ds}} = 2$ mV). (c) Energy diagrams of a Si DQD at the circle marked in (a) (the left diagram) and at the blue cross marked in (b) (the right diagram), where the valley degeneracy is assumed to be lifted. (d) The same diagram as (c) without an assumption that lifting of the valley degeneracy is small. Intradot and interdot tunnelings between different valleys are assumed to be weak so that the PSB is not lifted.

PSB features were observed at adjacent triple points, marked B, C, and D in Fig. 1(c). This is not expected for simple spin-$\frac{1}{2}$ PSB. Since the DQD has many electrons, spin-$\frac{3}{2}$ ground states can exist, leading to scenarios for consecutive PSB.[12] Blockade where valley degeneracy plays a role can also lead to consecutive PSB-like features. Even when a spin doublet is formed in DQDs, the current flow could be suppressed because of weak tunneling between valleys discussed above (see Appendix A).

B. Magnetic field dependence: Current dip

Figure 3(a) shows the leakage current in the PSB regime at triple point C in Fig. 1(c) as a function of magnetic field B applied normally to the DQD with a detuning, ϵ, corresponding to the arrow shown in the inset. A strong current dip was observed at $B = 0$, whereas the current with opposite bias does not change as a function of magnetic fields (see Appendix B). Similar current dips have been observed for DQDs in InAs nanowires[14,24] and carbon nanotubes[15] and can be attributed to spin-orbit induced relaxation,[25] which is suppressed at $B = 0$ due to a Van Vleck cancellation.[14,26] A Lorentzian line shape, $I_{\mathrm{fit}} = I_{\mathrm{max}}\{1 - 8B_{\mathrm{C}}^2/9(B^2 + B_{\mathrm{C}}^2)\}$ with characteristic width B_{C}, is predicted theoretically.[25] The squares in Fig. 3(b) correspond to the absolute values of the leakage current in the PSB regime along the dashed line in Fig. 3(a). Fits to the Lorentzian form [the blue curve in Fig. 3(b)] yield good agreement between theory and experiment. Furthermore, as the interdot tunneling between the two QDs is enhanced by changing V_{C}, the value of B_{C} extracted from the fit increases, as plotted in Fig. 3(c). This result is also consistent

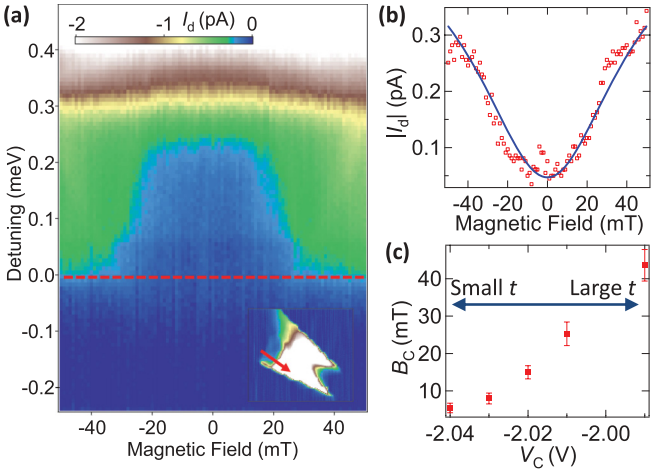

FIG. 3. (Color online) (a) Leakage current in the PSB regime as a function of magnetic field applied perpendicularly to the DQD and detuning, where $V_{ds} = -2$ mV, $V_{TG} = 0.97$ V, and $V_C = -1.99$ V. Inset: magnified plot of triple point C in Fig. 1(c), where the arrow corresponds to the detuning axis in the main figure. (b) Current along the dashed line in (a) denoted by the squares, and the fit to the data indicated by the blue line. (c) Values of B_C extracted from the fit as a function of V_C. Large V_C corresponds to a large interdot tunnel coupling t.

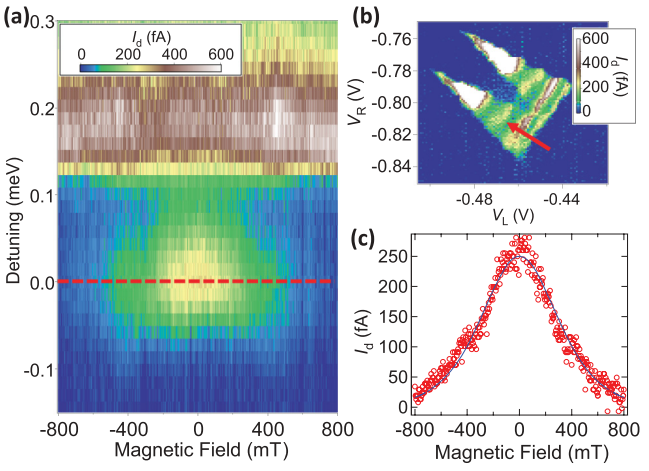

FIG. 4. (Color online) (a) Leakage current in the PSB regime as a function of magnetic field applied perpendicularly to the DQD and the detuning, where $V_{ds} = 2$ mV, $V_{TG} = 0.968$ V, and $V_C = -1.925$ V. (b) Magnified plot of triple point A in Fig. 1(c), where the arrow corresponds to the detuning axis in (a). (c) Current along the dashed line in (a) denoted by the circles, and the fit to the data indicated by the blue line.

with the theory, which predicts B_C proportional to interdot tunnel coupling.[25] These results suggest that spin-orbit effects dominate spin relaxation in these devices although spin-orbit interaction is usually weak in Si (see Appendix C).

Another possible mechanism leading to a dip in current leakage around $B = 0$ is spin-valley blockade with short-range disorder,[27] where the current dip as a function of magnetic-field-induced valley splitting is predicted. However, we have no independent evidence that the required B-dependent valley splitting exists. The physics of the valley in Si DQDs deserves further experimental and theoretical study.

C. Magnetic field dependence: Current peak

For some triple points, we observe a peak, rather than dip, in PSB leakage current on a larger field scale. As an example, the field dependence of the leakage current at triple point A in Fig. 1(c) is shown in Fig. 4(a). The arrow in the magnified plot of triple point A shown in Fig. 4(b) corresponds to the detuning axis in Fig. 4(a). Among the 15 triple points that show PSB [Fig. 1(c)], nine show a zero-field current dip and two show a peak. We also observed current peaks outside a current dip in some cases.

In GaAs DQDs, zero-field peaks in leakage current were attributed to hyperfine-induced spin relaxation.[13,28] However, the contribution of the hyperfine interaction should be small in Si systems, because the dominant ^{28}Si atoms have zero nuclear spin. Using 4.7% natural abundance of ^{29}Si and lithographic device dimensions gives an expected number N of nuclear spins in a Si DQD to be (2–3) $\times 10^4$, corresponding to a fluctuating Overhauser field magnitude $B_{nuc} = |A|/g\mu_B\sqrt{N} \sim 10$–$15$ μT, where μ_B is the Bohr magneton, the hyperfine coupling constant $|A| \sim 0.2$ μeV from NMR measurements[29,30] and $g \sim 2$ for electrons in Si. Since the peak width in Fig. 4(c) is larger than B_{nuc} by a factor of 10^4, the mechanism of the current peaks at $B = 0$ is not explained by hyperfine interaction.

Similar peaks were also seen in Si DQD in Ref. 19, where the peak is well described by spin-flip cotunneling.[31] When $k_BT > t$ (k_B is Boltzmann's constant and t is the interdot tunnel coupling), the spin-flip cotunneling current is given by $I_{cot} = 4ecg\mu_B B/3\sinh(g\mu_B B/k_BT)$ with $c = h\{[\Gamma_R/(\Delta-\epsilon)]^2 + [\Gamma_L/(\Delta+\epsilon-2U'-2eV_{ds})]^2\}/\pi$, where e is the electron charge, $\Gamma_{L(R)}$ is the coupling of the lead to the left (right) dot, Δ is the depth of the two-electron level,[32] and U' is interdot charging energy. Since we observed clear resonant tunneling peaks, $\Gamma_{L(R)}$ is larger than t.[33] In addition, if $\Gamma_{L(R)} > t > k_BT \sim 21$ μeV, the current would be much larger than the observed current shown in Fig. 4(b). As a result, $k_BT > t$ so that I_{cot} can be used to fit the current peak. The blue curve in Fig. 4(c) is I_{cot}, which has a good agreement with the data by using $T \sim 250$ mK, yielding $g \sim 2.3$ and $c \sim 54$ kHz/μeV. Since the current does not vary much along the base of the triangle in Fig. 4(b), we assume $\Gamma_L \sim \Gamma_R \equiv \Gamma$. By using expression of c with $\Delta \sim 1$ meV, $\epsilon \sim 0$ meV, $U' \sim 1$ meV, and $eV_{ds} \sim 2$ meV estimated from the bias triangle shown in Fig. 4(b), we extracted $\Gamma \sim 26$ μeV. Furthermore, t can be extracted to be about 0.3 μeV from the unblocked resonant tunneling peak current (~0.6 pA) with Eq. (15) in Ref. 21. These values are similar with those in Ref. 19 and in an experimentally reasonable range so that the spin-flip cotunneling processes are most likely the mechanism of the peak. It should be noted that, as for the dip in Fig. 3, spin-valley blockade with disorder could also explain the peak, but again we have at present no evidence of the required field-dependent valley splitting.[34]

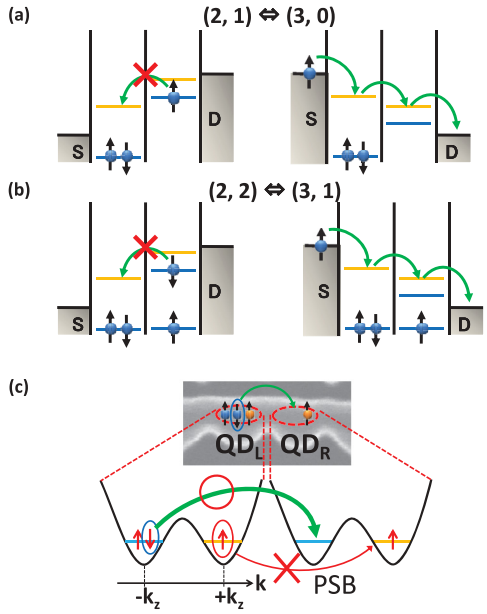

FIG. 5. (Color online) (a) and (b) Energy diagrams of a Si DQD where $(N_L, N_R) = (2,1)$ or $(3,0)$ in (a), and $(2,2)$ or $(3,1)$ in (b). The blue and yellow lines indicate different valleys. (c) Electron configuration for the $(3,1)$ regime in a Si DQD where doubly degenerate valleys are taken into account.

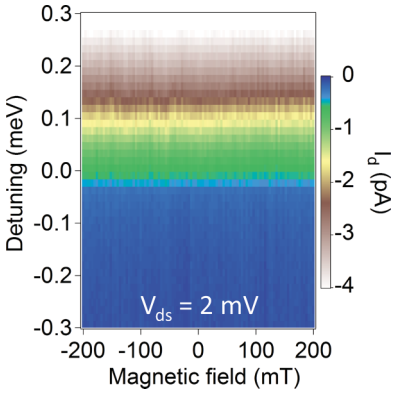

FIG. 6. (Color online) Magnetic field dependence of the current at triple point C, where $V_{ds} = 2$ mV, $V_{TG} = 0.97$ V, and $V_C = -1.99$ V. No dependences are observed.

ACKNOWLEDGMENTS

G.Y. and T.K. contributed equally to this work. We thank W. A. Coish, G. Burkard, A. Pályi, C. Barthel, J. Medford, and F. Kuemmeth for valuable discussions and K. Usami, T. Kambara, R. Suzuki, and T. Hiramoto for device fabrication. This work was partly supported by a Grant-in-Aid for Scientific Research from the Ministry of Education, Culture, Sports, Science, and Technology of Japan (No. 21710137, No. 19206035, and No. 22246040), JST-PRESTO, and Special Coordination Funds for Promoting Science and Technology. We thank DARPA-QuEST Program for partial support at Harvard.

APPENDIX A: VALLEY DEPENDENT BLOCKADE

We consider two typical blockades at $(2,1) \Leftrightarrow (3,0)$ and $(2,2) \Leftrightarrow (3,1)$, where the valley splitting is assumed to be small and tunneling between the different valleys is assumed to be weak.[23] Figure 5(a) shows the energy diagram of the first case. The blockade does not occur in the direction from $(3,0)$ to $(2,1)$ because the right-hand QD is empty. In the direction from $(2,1)$ to $(3,0)$, once two electron spins occupy one valley in the left-hand QD and an electron spin enters the same valley in the right-hand QD, no current flows because of the weak tunneling between different valleys. As a result, a blockade occurs for the same polarity as that of $(1,1) \Leftrightarrow (2,0)$ [see Fig. 2(d)]. Current blockade resulting from spin and valley degree of freedoms has been termed the spin-valley blockade,[35] which must play an important role for spin or valley qubits of Si.

Similarly, a blockade due to valleys occurs for the second case under negative bias polarity, as shown in Fig. 5(b). In contrast, current flow occurs for positive polarity because of doubly degenerate valleys. The $(3,1) \Rightarrow (2,2)$ transtion can be explained as follows. Figure 5(c) shows a typical $(3,1)$ state where doubly degenerate valleys which have different wave numbers ($+k_z$ and $-k_z$) are included. In the left QD, two spins occupy the $-k_z$ valley and a single up spin occupies the $+k_z$ valley, whereas a single up spin occupies the $+k_z$ valley in the right QD. In this case, a PSB occurs in the $+k_z$ valley, while the $-k_z$ valley in the right QD is empty so that one of the two spins in the left QD can move to the right QD. In other configurations, a spin in the left QD can also move to the right QD in a similar manner. As a result, current flow occurs in this condition, which is a possibility to explain our consecutive blockades. However, since this model does not fully explain the PSB patterns, further experimental studies of the PSB in a few-electron Si DQD are necessary.

APPENDIX B: NO MAGNETIC FIELD DEPENDENCE

Figure 6 shows the current at triple point C as a function of magnetic field B with a detuning. The bias direction is opposite to that in Fig. 3, where we did not observe a current dip.

APPENDIX C: ESTIMATION OF B_C

We do not know an accepted value for the spin-orbit length in a Si QD, l_{SO_Si} from the literature. On the other hand, the spin-orbit length of InAs QD, l_{SO_InAs}, has been reported, and is in the range 120–250 nm.[24,36] An estimate for l_{SO_Si} can be made by comparing only Rashba parts of l_{SO_Si} and l_{SO_InAs}, taking the Dresselhaus contribution in Si to be negligible because it is a nonpolar crystal.

The Rashba spin-orbit energy, E_{SO}, is given by[37]

$$E_{so} \propto \frac{eP^2}{3}\left[\frac{1}{E_g^2} - \frac{1}{(E_g + \Delta_{SO})^2}\right]\sigma \cdot k \times \langle E \rangle_v, \quad \text{(C1)}$$

where E_g is band gap, Δ_{SO} is spin-orbit splitting in the valence band, P is a band parameter related to the interband momentum matrix elements, σ is Pauli spin matrices, k is wave vector, and $\langle E \rangle_v$ is electric field. According to theory, P does not vary much between Si and InAs,[38] and $\langle E \rangle_v$, the electric field relevant for Rashba coupling, should be roughly the same size in the Si and InAs experiments because similar gate voltages

were used. Denoting as A the term in braces,

$$A = \frac{1}{E_g^2} - \frac{1}{(E_g + \Delta_{SO})^2}, \tag{C2}$$

we take $E_{g\_Si} = 1.1$ eV, $\Delta_{SO\_Si} = 0.044$ eV, $E_{g\_InAs} = 0.42$ eV, $\Delta_{SO\_InAs} = 0.38$ eV,[37] resulting in $l_{SO\_Si}/l_{SO\_InAs} \sim A_{InAs}/A_{Si} \sim 70$. Note that A_{InAs} may be smaller because $g \sim 8$ in the nanowire,[36] which is smaller than the bulk value ($g \sim 13$). As a result, we expect l_{SO_Si} to be in the range 1–10 μm.

Using estimated l_{SO_Si}, we estimate the value for B_C,[25]

$$B_C = \frac{2\sqrt{2}(1 + |\vec{\eta}|^2)t\sqrt{\Gamma_{rel}/\Gamma_{out}}}{\eta_x^2 + \eta_y^2}, \tag{C3}$$

where Γ_{out} is the rate of escape from the (0,2) singlet into the lead, $\Gamma_{rel} = I_{max}/4e$ is the spin relaxation rate, $\vec{\eta} = \vec{t_{SO}}/t$, and $\vec{t_{SO}}$ is the non-spin-conserving tunnel coupling due to spin-orbit interaction. For simplicity, we assume $\eta_x \sim \eta_y \sim \eta_z$, and $|\vec{\eta}| = |\vec{t_{SO}}|/t \sim l_{dot}/l_{SO}$ giving

$$B_C = \frac{2\sqrt{3}(1 + l_{dot}/l_{SO})t\sqrt{I_{max}/4e\Gamma_{out}}}{l_{dot}/l_{SO}}, \tag{C4}$$

where $l_{dot} = h/2\pi\sqrt{E_{orb}m_{eff}}$, m_{eff} is the effective mass in Si, $E_{orb} \sim 300$ μeV (experimentally measured value for the orbital level spacing), and $I_{max} \sim 0.5$ pA (again experimental value). B_C is plotted in Fig. 7. We note that the range of B_C is similar to that in Fig. 3 for this range of the parameters. While these estimates are rough, we believe they justify our interpretation that spin-orbit interaction plays an important role. The key point is that Rashba spin-orbit coupling is small, but not extremely small.

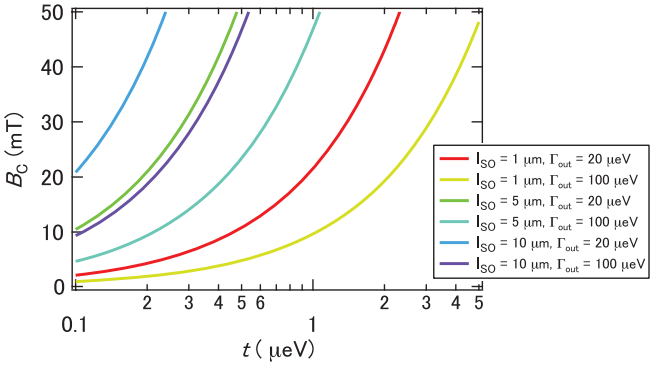

FIG. 7. (Color online) B_C versus t, where l_{SO} and Γ_{out} are parameters.

*Present address: Center for Quantum Devices, Niels Bohr Institute, University of Copenhagen, Universitetsparken 5, 2100 Copenhagen Ø, Denmark.

[1] D. Loss and D. P. DiVincenzo, Phys. Rev. A **57**, 120 (1998).
[2] F. H. L. Koppens *et al*. Nature (London) **442**, 766 (2006).
[3] J. R. Petta *et al*., Science **309**, 2180 (2005).
[4] M. Pioro-Ladriere *et al*., Nature Phys. **4**, 776 (2008).
[5] A. V. Khaetskii, D. Loss, and L. Glazman, Phys. Rev. Lett. **88**, 186802 (2002).
[6] H. O. H. Churchill, F. Kuemmeth, J. W. Harlow, A. J. Bestwick, E. I. Rashba, K. Flensberg, C. H. Stwertka, T. Taychatanapat, S. K. Watson, and C. M. Marcus, Phys. Rev. Lett. **102**, 166802 (2009).
[7] W. H. Lim *et al*., Appl. Phys. Lett. **94**, 173502 (2009).
[8] M. Xiao, M. G. House, and H. W. Jiang, Phys. Rev. Lett. **104**, 096801 (2010).
[9] Y. Hu *et al*., Nat. Nanotechnol. **2**, 622 (2007).
[10] C. B. Simmons *et al*., Phys. Rev. Lett. **106**, 156804 (2011).
[11] K. Ono, D. G. Austing, Y. Tokura, and S. Tarucha, Science **297**, 1313 (2002).
[12] A. C. Johnson, J. R. Petta, C. M. Marcus, M. P. Hanson, and A. C. Gossard, Phys. Rev. B **72**, 165308 (2005).
[13] F. H. L. Koppens *et al*., Science **309**, 1346 (2005).
[14] A. Pfund, I. Shorubalko, K. Ensslin, and R. Leturcq, Phys. Rev. Lett. **99**, 036801 (2007).
[15] H. O. H. Churchill *et al*., Nature Phys. **5**, 321 (2009).
[16] T. Kodera, K. Ono, Y. Kitamura, Y. Tokura, Y. Arakawa, and S. Tarucha, Phys. Rev. Lett. **102**, 146802 (2009).
[17] N. Shaji *et al*., Nature Phys. **4**, 540 (2008).
[18] H. W. Liu, T. Fujisawa, Y. Ono, H. Inokawa, A. Fujiwara, K. Takashina, and Y. Hirayama, Phys. Rev. B **77**, 073310 (2008).
[19] N. S. Lai *et al*., Sci. Rep. **1**, 110 (2011).
[20] G. Yamahata *et al*., Appl. Phys. Express **2**, 095002 (2009).
[21] W. G. van der Wiel *et al*., Rev. Mod. Phys. **75**, 1 (2003).
[22] L. P. Kouwenhoven *et al*., in *Mesoscopic Electron Transport*, edited by L. L. Sohn, G. Schon, and L. P. Kouwenhoven (Kluwer, Dordrecht, 1997), Vol. 345, pp. 105–214.
[23] D. Culcer, Ł. Cywiński, Q. Li, X. Hu, and S. Das Sarma, Phys. Rev. B **82**, 155312 (2010).
[24] S. Nadj-Perge, S. M. Frolov, J. W. W. vanTilburg, J. Danon, Y. V. Nazarov, R. Algra, E. P. A. M. Bakkers, and L. P. Kouwenhoven, Phys. Rev. B **81**, 201305(R) (2010).
[25] J. Danon and Y. V. Nazarov, Phys. Rev. B **80**, 041301(R) (2009).
[26] A. V. Khaetskii and Y. V. Nazarov, Phys. Rev. B **64**, 125316 (2001).
[27] A. Pályi and G. Burkard, Phys. Rev. B **82**, 155424 (2010).
[28] O. N. Jouravlev and Y. V. Nazarov, Phys. Rev. Lett. **96**, 176804 (2006).
[29] J. Schliemann, A. Khaetskii, and D. Loss, J. Phys.: Condens. Matter **15**, R1809 (2003).
[30] R. G. Shulman and B. J. Wyluda, Phys. Rev. **103**, 1127 (1956).
[31] W. A. Coish and F. Qassemi, Phys. Rev. B **84**, 245407 (2011).
[32] F. Qassemi, W. A. Coish, and F. K. Wilhelm, Phys. Rev. Lett. **102**, 176806 (2009).
[33] T. Fujisawa *et al*., Science **282**, 932 (1998).
[34] G. Burkard and A. Pályi (private communication).
[35] A. Pályi and G. Burkard, Phys. Rev. B **80**, 201404(R) (2009).
[36] C. Fasth, A. Fuhrer, L. Samuelson, V. N. Golovach, and D. Loss, Phys. Rev. Lett. **98**, 266801 (2007).
[37] R. Winkler, *Spin-Orbit Coupling Effects in Two-Dimensional Electron and Hole Systems* (Springer, Berlin, 2003).
[38] C. Tahan and R. Joynt, Phys. Rev. B **71**, 075315 (2005).